Proceedings of the
10th Graz Brain-Computer Interface Conference 2026

10.3217/978-3-99161-093-9-029

EEG-Based Detection of Continuous and Discrete Hand Movements for Cursor Control

Markus R. Crell[1], Gernot R. Müller-Putz[1,2]

[1]Institute of Neural Engineering, Graz University of Technology, Graz, Austria

[2]BioTechMed Graz, Graz, Austria

E-mail: gernot.mueller@tugraz.at

ABSTRACT: Continuous cursor control for non-invasive brain-computer interfaces (BCIs) has recently received widespread attention. However, the usability of such systems for patients with e.g., neuromuscular diseases remains limited while a selection mechanism is not simultaneously provided. We therefore attempt to asynchronously detect and discriminate between continuous and discrete hand movements to enable intuitive cursor control and click possibilities for cursor BCIs. Our results show that discrimination between discrete and continuous motions is possible with high accuracy and a low rate of false positive detections. We propose that the introduced method can be applied to non-invasive cursor control BCIs to add a click functionality to the cursor movement.

INTRODUCTION

An increasing share of everyday communication occurs through digital platforms, where effective interaction depends on the ability to move towards and select targets on a screen. For people with neuromuscular conditions such as amyotrophic lateral sclerosis (ALS), the ability for voluntary movement declines, resulting in an incapability to execute such movements. Brain–computer interfaces (BCIs) offer a promising approach to restore computer access under such circumstances. Using invasive recordings, the control of a computer cursor has been achieved recently [1, 2] and demonstrated the importance of such systems for the patient. However, invasive BCIs require surgery, which may not be feasible for all patients and requires an extensive preparation period prior to the implantation. Non-invasive, EEG-based BCIs offer an alternative for these patients and can be implemented with substantially less preparation effort [3]. In the non-invasive field, prior work has demonstrated the successful typing of words using a simple hand-movement-based click [4, 5] or paradigms such as code-modulated visual evoked potentials [6].

The detection of discrete hand movements from EEG can be achieved from low-frequency neural correlates of motion, so called movement-related cortical potentials (MRCPs). MRCPs are changes in the EEG especially over central motor regions that emerge prior to and during a movement. They show a gradual, negative shift beginning up to two seconds prior to movement onset, followed by a return to baseline [7]. Since the occurrence of MRCPs is independent of visual cues, these signals are well suited to detect self-paced motions. Prior work has demonstrated the successful asynchronous detection of MRCPs with the help of machine learning methods such as shrinkage linear discriminant analysis (sLDA) [4, 8, 9] or random forest classifiers [10].

Recent studies have also focused on the continuous control of computer cursors from non-invasive neural signals. These studies demonstrated that continuous motion and direction can be decoded successfully from electroencephalography (EEG) data [11–14]. While some studies demonstrated successful decoding of continuous movement from low-frequency components [14, 15], other studies showed high frequencies to encode continuous movement speed [16, 17].

Specifically, changes in oscillatory components relative to (continuous) movement occur in mu and beta frequency bands. Such changes in oscillatory components relative to a specific event have been described as event-related (de-)synchronization (ERD/S). During movement planning and execution, oscillatory power in the mu and beta bands shows event-related desynchronization (ERD) that persists until the movement ends [18, 19]. At termination, this desynchronization is followed by a transient increase in beta synchronization before returning to baseline, a phenomenon known as post-movement beta synchronization. Prior studies have also identified this pattern for continuous hand movements and utilized it to decode continuous hand movement [20]

Besides recent advances for cursor control BCIs, the practical use of continuous movement decoding for cursor control remains limited when systems provide only continuous cursor movement without a reliable selection mechanism. While dwell-time selection is possible based on cursor stopping, in everyday usage, dwell-time selection often slows communication. Based on prior work [4, 8, 16], we therefore investigate the discriminability between continuous and discrete hand motions to enable simultaneous cursor control and selection through clicks.

 10.3217/978-3-99161-093-9-029

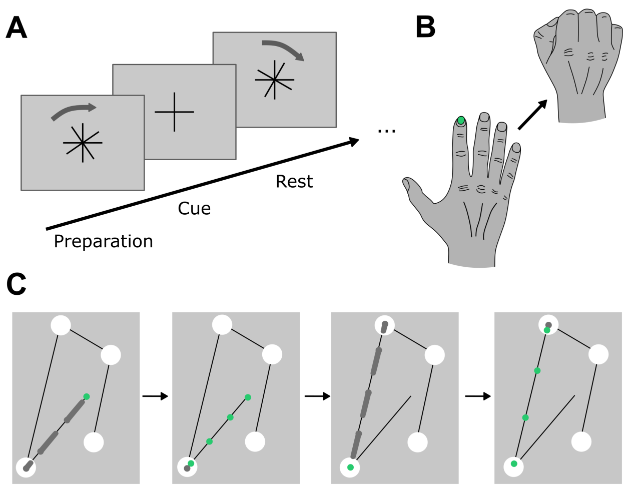

Figure 1: Paradigms and hand motion for calibration data collection. (A) Rotational cross used to collect discrete movement data. The overlap of the rotational cross with the static cross (cue) prompts the participant to execute the specified hand movement. (B) The hand movement that is executed whenever the two crosses overlap. (C) Continuous movement paradigm. The green cursor is controlled by the movement of the index finger of the participant. The grey cursor prompts the movement between the white dots (targets).

We aim to achieve a similar rate of true positives and false positives for the click detection as well as a similar continuous movement detection accuracy for the combined decoding as for individual tasks. We hypothesize that a differentiation between discrete, short and continuous motions can be achieved by leveraging different frequency components of the EEG based on the prolonged ERD/S patterns during continuous movement compared to the occurrence of low-frequency MRCPs at the movement onset of discrete motions.

MATERIALS AND METHODS

Experimental Paradigm: Five participants (3 male, 2 female) with a mean age of 29.2 ± 3.4 years took part in two consecutive EEG measurements. At the beginning of each measurement, participants positioned their right hand on a table with the palm facing downwards.

The first paradigm (adopted from [8, 21]) consisted of a static fixation cross overlayed by a rotating cross (Figure 1 A). The rotating cross rotated at different speeds. Participants were instructed to execute a short hand motion whenever two crosses overlapped (cue). This motion consisted of a flexion of the fingers and the thumb of the right hand as well as the wrist, followed by a return to the initial resting position (Figure 1 B). The first paradigm comprised three runs, each of which had a duration of 334 s. During each run, participants executed 100 discrete hand motions. The inter-trial interval ranged between 2.5 and 4.75 s.

The second paradigm comprised six runs of ten continuous start-and-stop movements each. A start-and-stop movement (Figure 1 C) was designed around a fixed number of targets with black lines between the targets showing the intended movement pattern. Targets and trajectories together formed the target-trajectory. The timing of the movement was cued by a grey cursor, while participants controlled a green cursor that was mapped to the screen based on a tracked marker on the participants index finger. Both the grey and the green cursor started in the middle of the screen. When the grey cursor moved towards the first target position, participants waited until the grey cursor had reached the first target. The grey cursor paused its movement at the target and the participant moved the green cursor along the black line towards the first target. The grey cursor then continued towards the next target, during which the participants waited at the previous position. This procedure was repeated until the grey and green cursor reached the last target, after which a different target-trajectory was displayed. Participants started each trial at a fixed starting position and returned to that position as soon as a new target-trajectory was displayed. The number of targets (three to seven) as well as their position on the screen was pseudo-randomly selected, resulting in differing trial durations. However, the target-trajectories were similar for each participant. On average, trials had a duration of 30.6 ± 5.8 s. Out of the duration of one trial, on average 18 % were spent executing a continuous movement while the rest was spent waiting for the next motion.

Prior to the two paradigms, participants executed an eye-movement paradigm [22] during which they performed left/right and up/down eye movements. The data collected during this paradigm was used to eliminate eye artifacts from the EEG.

Data Acquisition and Feature Extraction: We measured the EEG of participants from 60 electrodes positioned according to a standard 10-10 montage. Electrooculography (EOG) was recorded from four electrodes positioned on the outer canthi of the eyes as well as above and below the left eye. EOG and EEG was recorded using a biosignal amplifier (BrainAmp, Brain Products GmbH, Gilching, Germany) at a sampling rate of 500 Hz. Participants were further equipped with a motion capture marker positioned on the index finger of the right hand. Movements of the marker were recorded at a rate of 30 Hz using a custom motion capture system.

EEG and EOG data was first bandpass filtered between 0.3 and 70 Hz (Butterworth filter, 4^{th} order). Eye-artifacts were eliminated using the SGEYESUB algorithm [22] and EOG channels were subsequently removed from the data. To extract the movement onset of discrete hand motions and the start and stop of continuous movements, we extracted the movement speed of the index finger from the positions of the motion capture marker. We then applied a threshold to the speed and aligned the movement data to the neural data.

Two sets of features were extracted: low-frequency features were obtained by lowpass-filtering the EEG to 3.5 Hz (Butterworth filter, 4^{th} order) and downsampling

10.3217/978-3-99161-093-9-029

the data to 10 Hz. Broadband-frequency features were obtained by lowpass-filtering the EEG to 40 Hz (Butterworth filter, 4^{th} order) and downsampling the data to 125 Hz.

Discrete Movement Detection (First Paradigm): The detection of discrete movements from the first paradigm focused on the detection of the movement onset of the discrete motion as obtained with the motion capture system. We attempted to detect movement onsets from windows of low-frequency features using an sLDA. To improve detection performance, we applied a hyperparameter search over the windowlength w_l and the additional detection delay d as described in [4]. For each participant, we calibrated a model for the detection of movement onsets on the data from the first paradigm. We selected the optimal windowlength and detection delay from $w_l \in [0.1; 2.0]$, $d \in [-min(1.1, w_l); 0.0]$ based on the maximum Matthews correlation coefficient (MCC) [23] of the validation set. The MCC is a metric for the evaluation of binary classification and is robust to class-imbalance, as is often the case in asynchronous BCIs. Movement onset predictions were regarded as true positives if they occurred up to -0.2 s prior or up to 0.8 s after the actual movement onset. We further applied a refractory period of 1.0 s after each movement onset detection to eliminate accidental multiple detections. For each model calibrated during the hyperparameter search, the detection probability threshold p was tuned to allow for not more than 2.0 false positives per minute (FP/min) based on the validation set. We selected the highest p for which this condition was true. The final detection performance was evaluated on the test set by calculating the MCC, the true positive rate (TPR) and FP/min. To obtain a higher confidence on the test set performance, we applied a three fold cross-validation procedure. Specifically, we generated three folds of the same size where each fold was treated as training, validation or test set exactly once. The same three-fold cross-validation procedure was also applied to all subsequent models.

Continuous Movement Decoding (Second Paradigm): We decoded continuous movement from windows of the broadband-frequency features of the data from the second paradigm. The ground truth of the continuous movement was obtained from the movement speed of the right hand measured with the motion capture system. For this, we employed a CNN-LSTM neural network. The architecture of the CNN was based on the EEGNet architecture [24], which has been designed to extract relevant frequency bands and has been shown to enable speed decoding for continuous movements [16]. The inclusion of an LSTM has been shown to increase performance in EEG-based continuous movement tasks [25]. Similar to the discrete movement detection, we applied a three-fold cross validation procedure and hyperparameter search over the windowlength w_l, the additional detection delay d and the detection threshold p. We calibrated a model for each participant on the data from the second paradigm and selected the optimal hperaparameters based on the MCC of the validation set. The final performance was evaluated on the test set by calculating the MCC, the TPR and the false positive rate (FPR). In contrast to the discrete movement detection, we did not apply a refractory period.

Combined Discrete and Continuous Movement Decoding: The detection of discrete and the decoding of continuous movements was achieved by applying the described procedures for both models to the data of both paradigms. Specifically, we applied each the discrete detection and continuous decoding on the separate datasets from the first and second paradigm. For the discrete movement detection, the labels of the continuous movement in the dataset from the second paradigm were eliminated. For the continuous movement decoding, the labels of the discrete motions in the dataset from the first paradigm were eliminated. For the combined continuous and discrete models, the complete three-fold cross-validation procedure and hyperparameter search was repeated for both models on the combined datasets and each participant. We finally applied the optimal models to the same test sets and evaluated the performance of the combined predictions. In addition to the refractory period of the discrete detection, we also applied a refractory period to the continuous movement decoding after each discrete movement onset detection. Specifically, we inhibited any continuous movement detection through a refractory period of 3.0 s after the detection of a discrete movement onset.

We compared the performance of the discrete movement detection on the data from the first paradigm with the performance on the combined data and similar for the continuous movement decoding. Additionally, we evaluated the rate of FP/min and the MCC, TPR and FPR of the combined decoding approach solely on the parts of the data corresponding to the first and second paradigm, so that we were able to directly compare the performance.

RESULTS

When calibrating models for the discrete movement detection on the data from the first paradigm and evaluating the model on data from the first paradigm (*discrete movement - single decoding*), we achieved an average TPR of the discrete movement detection of 49.09 ± 20.55 % (mean $\pm$ standard deviation) with an average rate of FP/min of 2.83 ± 0.48. The mean MCC was 0.58 ± 0.18. For the continuous movement decoding calibrated and evaluated only on data from the second paradigm (*continuous movement - single decoding*), the average MCC was 0.59 ± 0.10. With the combined approach, models for the discrete movement detection that were calibrated and evaluated on the data from both paradigms (*discrete movement - combined decoding*) achieved an average TPR of 48.03 ± 21.32 % (-1.06 % compared to *discrete movement - single decoding*) with an average rate of FP/min of 1.92 ± 0.63 (-0.91 compared to *discrete movement - single decoding*) and an MCC of 0.53 ± 0.21 (-0.05 compared to *discrete movement - single decod-*

 10.3217/978-3-99161-093-9-029

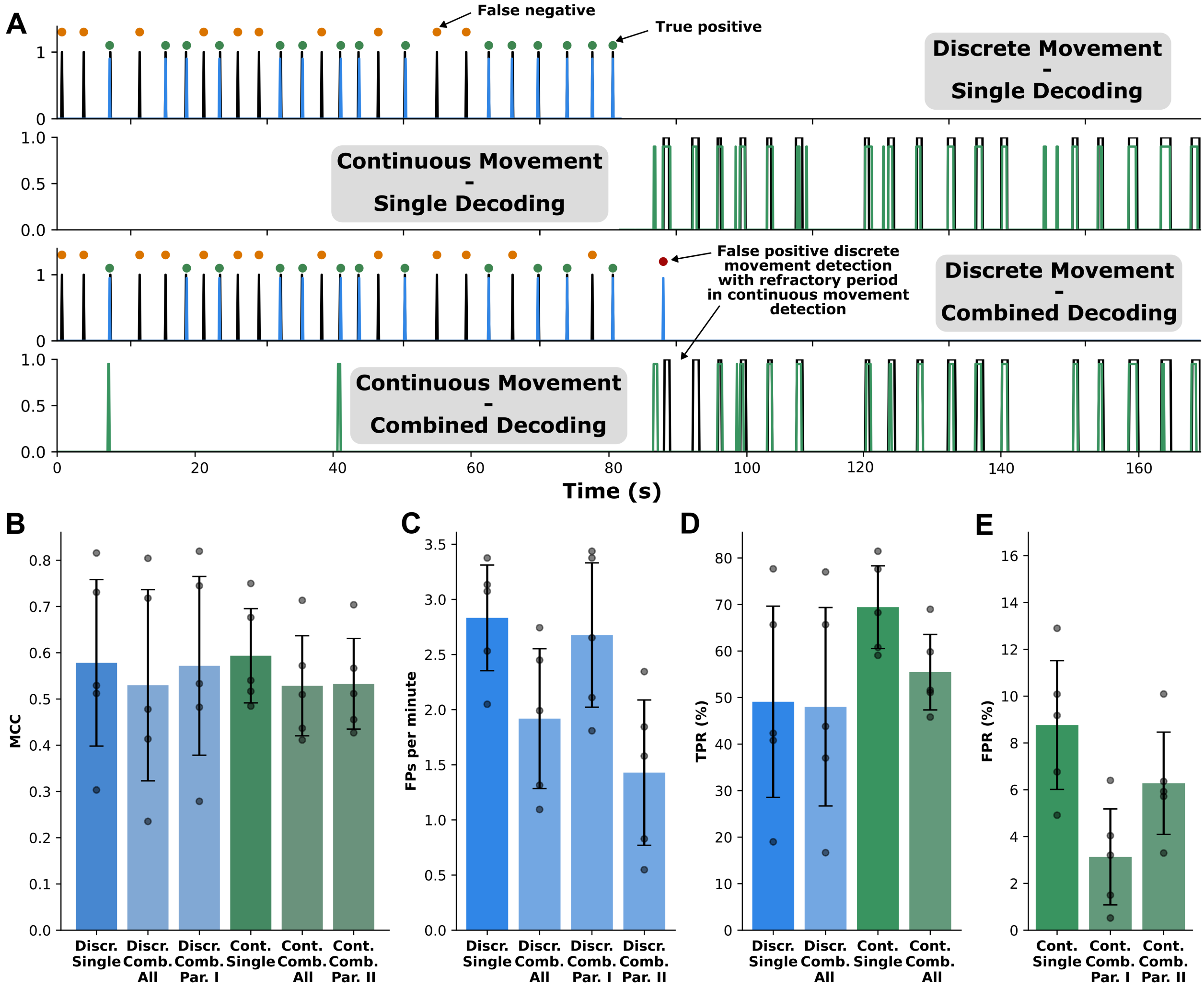

Figure 2: (A) Executed (black) and decoded (blue: discrete, green: continuous) discrete and continuous movement patterns. The upper graph shows parts of the data from the first paradigm with movement detections based on the optimal model calibrated only on the data from the first paradigm (discrete movement - single decoding). The second graph shows parts of the data from the second paradigm with continuous movements decoded based on the optimal model calibrated only on the data from the second paradigm (continuous movement - single decoding). The third and fourth graphs show the combined decoding output from the discrete and continuous models. Output from the discrete movement detection model is shown in the upper graph together with the executed motions while output from the continuous model is shown in the lower graph together with the executed movements. False positives (red), true positives (green) and false negatives (yellow) are shown for the discrete movement detection as dots. (B) MCCs for the different models (discrete and continuous) calibrated on the single or combined data and evaluated on the different paradigms. Black dots indicate values for individual participants. (C) Rate of FP/min for the discrete model calibrated and evaluated on the different paradigms. (D) TPR of the discrete and continuous model calibrated and evaluated on the different paradigms. (E) FPR of the continuous model calibrated and evaluated on the different paradigms.

ing). When evaluating these models only on the data from the first paradigm (*discrete movement - combined decoding - paradigm I*), we achieved an average rate of FP/min of 2.68 ± 0.65 (-0.15 compared to *discrete movement - single decoding*) and an MCC of 0.57 ± 0.19 (-0.01 compared to *discrete movement - single decoding*). The rate of FP/min of the *discrete movement - combined decoding - paradigm II* was on average 1.43 ± 0.66.

For the continuous movement decoding, models that were calibrated and evaluated on the data from both paradigms (*continuous movement - combined decoding*) achieved an average MCC of 0.53 ± 0.11. When evaluating these models only on the data from paradigm two (*continuous movement - combined decoding - paradigm II*), we achieved an average MCC of 0.53 ± 0.10 (-0.06 compared to *continuous movement - single decoding*).

For the *continuous movement - single decoding* model, the TPR, ie. the rate of actual movement that was identified as movement, was $69.43 \pm 8.88\,\%$, while the FPR, i.e. the rate of rest that was falsely identified as movement, was $8.77 \pm 2.75\,\%$. For the *continuous movement - combined decoding - paradigm I*, the FPR was

 10.3217/978-3-99161-093-9-029

$3.13 \pm 2.05\,\%$. For the *continuous movement - combined decoding - paradigm II*, the TPR was $55.45 \pm 8.11\,\%$ ($-13.98\,\%$ compared to *continuous movement - single decoding*) while the FPR was $6.28 \pm 2.18\,\%$ ($-2.49\,\%$ compared to *continuous movement - single decoding*).

Figure 2 A shows parts of the paradigms and decoding results for one participant. The first two graphs show the detected discrete motions (blue) and the executed movements (black) for the first paradigm (*discrete movement - single decoding*) and the detected continuous movements (green) and executed movements (black) for the second paradigm (*continuous movement - single decoding*). The lower graphs show the decoding results of the combined decoding approach split into the detected discrete movements during both paradigms (*discrete movement - combined decoding*) and the detected continuous movements during both paradigms (*continuous movement - combined decoding*). The reported results for the different models and evaluation modes are shown in Figure 2 B for the MCC, Figure 2 C for the rate of FP/min, Figure 2 D for the TPR and Figure 2 E for the FPR.

DISCUSSION

The simultaneous detection of discrete and continuous hand movements for the utilization in cursor BCIs is of great relevance for the usability of cursor BCIs in motor-impaired patients. The current study shows that the asynchronous detection and differentiation of continuous and discrete movement is possible with only slight decreases of the performance compared to detecting only discrete or continuous movement.

Specifically, the TPR of the discrete movement onset detection was reduced minimally in the combined decoding approach. Similarly, the MCC was reduced only slightly for the discrete detection of movement. However, there was a substantial decrease in detected false positives per minute when evaluating both paradigms together, which was largely driven by a low rate of false positives during the second paradigm. This indicates that the model rarely detected any discrete motions during continuous movements.

The decoding of continuous movement demonstrated a higher reduction in the MCC. Specifically, the TPR dropped by nearly $14\,\%$ when training the model on data from both paradigms. Simultaneously, the FPR also decreased. The occurrence of falsely decoded continuous movement was especially low during the first paradigm, indicating that discrete motions were rarely mistaken as continuous movements.

Overall, the detection performances of both the discrete and continuous model were only slightly reduced when trained and evaluated on data from both paradigms compared to the single paradigms. False detection rates remained sufficiently low in the corresponding original paradigms and were even reduced during the other paradigm, i.e., the rate of false positive detections of discrete motions in the second paradigm was even lower than that in the first paradigm and similar for the continuous decoding.

Prior studies have shown that the rate of false positives that was achieved during the discrete motion detection is suitable for spelling five-letter words in a row-column scanner [4]. Thus, we assume that the false positive rates would not hinder the participant during the application of the cursor BCI. Further, the introduced refractory periods of 1 s for discrete movements and 3 s of inhibited continuous movement after a detected discrete movement are sufficiently low to allow for high-performance control of computers.

CONCLUSION

The presented results demonstrate that the asynchronous detection of continuous hand movement and discrete hand motions can be achieved simultaneously with sufficient differentiation between the actions. The low rates of false positive detections of discrete motions during continuous movement and vice versa demonstrates the feasibility of the proposed method. Thus, the proposed method could be utilized in a cursor control BCI to move the cursor and make selections on a screen without needing to hover over the target. We believe that these results are an important step towards a fully functional cursor control BCI that can be applied in patients with neuromuscular conditions.

Limitations of the current study mainly concern the sample size of participants and the separated data collection. Since data for the discrete movements was collected separately from the continuous movements, it is not certain that the decoder performances can be transferred to real-world scenarios. Future work should therefore focus on a paradigm which combines continuous movement and clicks. Further, the online application of the method was not evaluated. This is an important step to identify further issues and test whether the method is suited for an online BCI for patients and will be pursued in future work.

ACKNOWLEDGEMENTS

This project is funded by the European Union's HORIZON-EIC-2021-PATHFINDER CHALLENGES program under grant agreement No 101070939 and by the Swiss State Secretariat for Education, Research and Innovation (SERI) under contract number 22.00198.

REFERENCES

[1] Wilson GH *et al.* Long-term unsupervised recalibration of cursor-based intracortical brain–computer interfaces using a hidden Markov model. Nature Biomedical Engineering. 2025:1–19.

[2] Deo DR, Willett FR, Avansino DT, Hochberg LR, Henderson JM, Shenoy KV. Brain control of bimanual movement enabled by recurrent neural networks. Scientific Reports. 2024;14(1):1598.

10.3217/978-3-99161-093-9-029

[3] Edelman BJ *et al.* Non-invasive Brain-Computer Interfaces: State of the Art and Trends. IEEE Reviews in Biomedical Engineering. 2024;PP(99):1–25.
[4] Crell MR, Kostoglou K, Suwandjieff P, Cruz JRD, Muller-Putz GR. A non-invasive, MRCP-based BCI for online communication. IEEE Transactions on Neural Systems and Rehabilitation Engineering. 2026;PP(99):1–1.
[5] Scherer R *et al.* Thought-based row-column scanning communication board for individuals with cerebral palsy. Annals of Physical and Rehabilitation Medicine. 2015;58(1):14–22.
[6] Martínez-Cagigal V, Thielen J, Santamaría-Vázquez E, Pérez-Velasco S, Desain P, Hornero R. Brain–computer interfaces based on code-modulated visual evoked potentials (c-VEP): a literature review. Journal of Neural Engineering. 2021;18(6):061002.
[7] Shibasaki H, Hallett M. What is the Bereitschaftspotential? Clinical Neurophysiology. 2006;117(11):2341–2356.
[8] Crell MR, Kostoglou K, Sterk K, Müller-Putz GR. A novel paradigm for fast training data generation in asynchronous movement-based BCIs. Frontiers in Human Neuroscience. 2025;19:1540155.
[9] Ofner P, Schwarz A, Pereira J, Müller-Putz GR. Upper limb movements can be decoded from the time-domain of low-frequency EEG. PLoS ONE. 2017;12(8):e0182578.
[10] Liu D *et al.* EEG-Based Lower-Limb Movement Onset Decoding: Continuous Classification and Asynchronous Detection. IEEE Transactions on Neural Systems and Rehabilitation Engineering. 2018;26(8):1626–1635.
[11] Lu X *et al.* Electroencephalography Enables Continuous Decoding of Hand Motion Angles in Polar Coordinates. Cyborg and Bionic Systems. 2026;7:0469.
[12] Mondini V, Sburlea AI, Müller-Putz GR. Towards unlocking motor control in spinal cord injured by applying an online EEG-based framework to decode motor intention, trajectory and error processing. Scientific Reports. 2024;14(1):4714.
[13] Pulferer HS, Ásgeirsdóttir B, Mondini V, Sburlea AI, Müller-Putz GR. Continuous 2D trajectory decoding from attempted movement: across-session performance in able-bodied and feasibility in a spinal cord injured participant. Journal of Neural Engineering. 2022;19(3):036005.
[14] Mondini V, Kobler RJ, Sburlea AI, Müller-Putz GR. Continuous low-frequency EEG decoding of arm movement for closed-loop, natural control of a robotic arm. Journal of Neural Engineering. 2020;17(4):046031.
[15] Kobler RJ, Sburlea AI, Mondini V, Hirata M, Müller-Putz GR. Distance- and speed-informed kinematics decoding improves M/EEG based upper-limb movement decoder accuracy. Journal of Neural Engineering. 2020;17(5):056027.
[16] Crell MR, Müller-Putz GR. Handwritten character classification from EEG through continuous kinematic decoding. Computers in Biology and Medicine. 2024;182:109132.
[17] Lv J, Li Y, Gu Z. Decoding hand movement velocity from electroencephalogram signals during a drawing task. BioMedical Engineering OnLine. 2010;9(1):64.
[18] Pfurtscheller G, Silva FLd. Event-related EEG/MEG synchronization and desynchronization: basic principles. Clinical Neurophysiology. 1999;110(11):1842–1857.
[19] Pfurtscheller G, Solis-Escalante T. Could the beta rebound in the EEG be suitable to realize a “brain switch”? Clinical Neurophysiology. 2009;120(1):24–29.
[20] Crell MR, Müller-Putz GR. Detection of motion termination from EEG during the execution of continuous hand movement. Proceedings of the 9th Graz Brain-Computer Interface Conference 2024. 2024:139–144.
[21] Suwandjieff P, Müller-Putz GR. EEG Analyses of visual cue effects on executed movements. Journal of Neuroscience Methods. 2024;410:110241.
[22] Kobler RJ, Sburlea AI, Lopes-Dias C, Schwarz A, Hirata M, Müller-Putz GR. Corneo-retinal-dipole and eyelid-related eye artifacts can be corrected offline and online in electroencephalographic and magnetoencephalographic signals. NeuroImage. 2020;218:117000.
[23] Chicco D, Jurman G. The advantages of the matthews correlation coefficient (mcc) over f1 score and accuracy in binary classification evaluation. BMC Genomics. 2020;21.
[24] Lawhern VJ, Solon AJ, Waytowich NR, Gordon SM, Hung CP, Lance BJ. EEGNet: a compact convolutional neural network for EEG-based brain–computer interfaces. Journal of Neural Engineering. 2018;15(5):056013.
[25] Chen YF *et al.* Continuous Bimanual Trajectory Decoding of Coordinated Movement From EEG Signals. IEEE Journal of Biomedical and Health Informatics. 2022;26(12):6012–6023.